Minerals Engineering 235 (2026) 109797

Contents lists available at ScienceDirect

Minerals Engineering

journal homepage: www.elsevier.com/locate/mineng

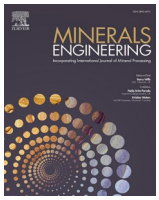

Performance evaluation of gold (III) bio-reduction by bacterial strains and a consortium isolated from gold mine effluent

Miranda Mpeta *, Job T. Tendenedzai, Shepherd M. Tichapondwa, Evans M.N. Chirwa

Water Utilisation and Environmental Engineering Division, Department of Chemical Engineering, University of Pretoria, Pretoria 0002, South Africa

ARTICLE INFO

Keywords:
Bio-reduction
Bio-recovery
Adapted strains
Consortium
Au (III)
Gold nanoparticles

ABSTRACT

The bioreduction of Au (III) to Au (0) offers a sustainable and eco-friendly alternative to conventional gold recovery methods, reducing environmental impacts associated with chemical processing. This study investigated the bioreduction capabilities of indigenous bacterial strains and a microbial consortium isolated from gold tailings and mine wastewater. Aerobic batch experiments were conducted at pH 7 and 35 ± 2°C over 24 h, with initial Au (III) concentrations of 3 and 6 ppm, to compare the reduction efficiencies of individual strains and a mixed consortium. Gram-negative bacteria (*Stenotrophomonas maltophilia, Klebsiella pneumoniae, Acinetobacter bereziniae*) achieved superior reduction efficiencies of 98.33–99.8 %, outperforming the Gram-positive *Bacillus cereus* (92.9 %), likely due to differences in cell wall structure, with Gram-negative strains leveraging outer membrane proteins and efficient extracellular electron transfer mechanisms, while *B. cereus* relies on biosorption via its thicker peptidoglycan layer. The consortium, combining all four strains, reached 94.5 % efficiency, reflecting synergistic interactions through resource partitioning and metabolite recycling. Scanning electron microscope (SEM), Energy-dispersive X-ray spectroscopy (EDS), X- ray diffraction (XRD) and X-ray photoelectron spectroscopy (XPS) confirmed the formation of Au (0) nanoparticles, with an 8.5 % crystalline gold content in the consortium despite low starting concentrations. These findings highlight the potential of indigenous bacteria for efficient gold bio- recovery from mining effluents and tailings, demonstrating a viable bio- hydrometallurgical process that integrates waste treatment with precious metal extraction. The technology offers significant advantages for mining operations through reduced chemical consumption, lower energy requirements, and simultaneous environmental remediation, supporting the industry's transition toward sustainable extraction practices and circular resource utilization in mineral processing operations.

1. Introduction

Gold (Au) exists in various oxidation states, with gold (III)/ (Au (III)) being a highly toxic ionic form. Au (III), also referred to as auric gold is the more stable species of gold other than the aurous form, Au (Nicol et al., 1987; Söhnel et al., 2001). This oxidation state often arises in the context of industrial applications and mining activities, where gold is extracted and processed. Au (III) can leach into surrounding environments because of these operations and due to its high solubility in water, particularly in chloride-rich environments, increasing its mobility in surface and groundwater systems (Nicol et al., 1987). This leads to significant ecological challenges such as inhibition of microbial growth and enzymatic activity, affecting nutrient cycling in ecosystems (Reith et al., 2006). In terrestrial environments, Au (III) in contaminated soils can reduce plant growth and microbial diversity, altering soil functionality (Reith et al., 2007). Gold mining, particularly artisanal and small-scale mining, generates significant amounts of Au (III)-containing wastewater and tailings. Improper disposal of these effluents can contaminate rivers, lakes, and groundwater, affecting drinking water quality and agricultural productivity. The gold (III) ions found in gold mine tailings and leachate are typically in the range of 0.1–0.5 g/t (Ubaldini et al., 2019). Apart from the mine waste, growing volumes of electronic waste (e-waste) containing gold contributes to Au (III) release during recycling processes. Acidic leaching techniques used to recover gold from e-waste can generate Au (III)-rich effluents (Cui & Zhang, 2008), which, if mismanaged, contaminate soil and water bodies. This is a significant concern in urban environments with inadequate waste management systems and an opportunity for resource recovery.

* Corresponding author.
E-mail addresses: u24054276@tuks.co.za (M. Mpeta), job.tendenedzai@tuks.co.za (J.T. Tendenedzai), shepherd.tichapondwa@up.ac.za (S.M. Tichapondwa), evans.chirwa@up.ac.za (E.M.N. Chirwa).

https://doi.org/10.1016/j.mineng.2025.109797
Received 8 June 2025; Received in revised form 16 September 2025; Accepted 20 September 2025
Available online 24 September 2025

Though generated in low concentrations, gold nanoparticles have an attractive market value and have in recent years been used for other critical applications such as in the medical field, electronics, paints, and catalysis, among others (Chaturvedi et al., 2012). Biocatalysis using various bacterial species has emerged as promising avenues for the recovery and synthesis of gold nanoparticles in an eco-friendly manner.

Several soil microorganisms, including bacteria, have demonstrated versatility in the bioreduction of gold ions, enabling the biosynthesis of gold nanoparticles (AuNPs). For example, *Acinetobacter* strains GWRVA25 and SW30 produced extracellular AuNPs from $HAuCl_4$, with GWRVA25 forming monodispersed spherical particles (~15 nm) and SW30 generating either spherical (~19 nm) or polyhedral (~39 nm) particles depending on cell density. *Pseudomonas aeruginosa* showed pH-dependent morphology, yielding spherical AuNPs at pH 7 and nanoplates at pH 4, while *Rhodopseudomonas capsulata* formed spherical particles at neutral pH and larger structures under more acidic conditions (Husseiny et al., 2007).

Deinococcus radiodurans, notable for its resistance to oxidative stress, synthesized AuNPs both intracellularly and extracellularly within two hours (Li et al., 2016). *Bacillus subtilis* also produced AuNPs using thiol-rich peptides as reducing agents(Thirumurugan et al., 2012). Collectively, these findings underscore the diversity of microbial systems in AuNP biosynthesis, with synthesis conditions such as pH, temperature, and cell density strongly influencing nanoparticle size, shape, and functionality.

Microorganisms that have been used for bio-reduction utilize different mechanisms (El-Sayed et al., 2021; Li et al., 2011). In a bioreduction process, mediated by sulfur-containing compounds, bioreduction occurred both extracellularly and intracellularly, reflecting a robust microbial adaptation to metal stress (Liu et al., 2018). Possible mechanisms of bioreduction include enzymatic activity, secreted metabolites and cell wall interaction (Baserisalehi et al., 2017). In the case of gold bio-reduction, the mechanism primarily involves the interaction of Au (III) with biomolecules within the bacterial cells, leading to the stabilization and reduction of Au (III) to Au (0).

Research indicates that gold ions can interact favorably with sulfur or nitrogen ligands present in the cell wall and cytoplasmic matrix, acting as electron donors during the reduction process (Gardea-Torresdey et al., 2000; Maeda & Tsuruta, 2020).

While several studies have explored the bioreduction capabilities of individual bacterial strains, the role of naturally occurring microbial consortia remains underexplored. Many existing studies rely on pure cultures, which, while useful as models, do not reflect the complexity of real environments like gold mine tailings. These environments host diverse microbial communities, often including Proteobacteria, Firmicutes, and Actinobacteria, that interact under extreme conditions. Such consortia can exhibit synergistic effects, enhancing metal reduction efficiency, process stability, and resilience. However, comparative studies evaluating individual strains versus consortia in Au (III) reduction are still limited.

This study aimed to assess the bioreduction efficiency of locally adapted bacterial strains and a microbial consortium derived from gold tailings with particular focus on their biocatalytic properties in transforming Au (III) to Au (0). The investigation explores how these microorganisms function as natural biocatalysts, leveraging their enzymatic machinery to accelerate the reduction of soluble gold ions into solid metallic gold under environmentally relevant conditions. By comparing reduction performance, gold recovery potential, and nanoparticle formation, it offered insights into the feasibility of microbial systems for sustainable gold recovery and mine wastewater treatment, while also exploring the underlying biochemical mechanisms involved. Biocatalysis, driven by enzymatic reduction and cell-surface interactions, underpins this process, with metabolites such as glucose providing the driving power.

Additionally, the bioreduction of gold (III) to elemental gold using bacterial strains and microbial consortia, as investigated in this study, significantly contributes to multiple Sustainable Development Goals (SDGs 6, 9 and 12) by promoting eco-friendly resource recovery and pollution mitigation, fostering circular economy principles. It also offers a low-energy alternative to conventional gold recovery methods, collectively enhancing environmental sustainability and responsible resource management.

2. Materials and methods

2.1. Growth media

Tryptone Soya Agar (TSA) was prepared by dissolving 40 g in 1 L of distilled water and covered. Tryptone Soya Broth (TSB) was prepared by dissolving 30 g in 1L of distilled water. Both were manufactured by Oxoid Ltd., Basingstoke, Hants, UK. After preparation, both were sterilized via autoclaving (121 °C, 15 min).

2.2. Mineral salt medium preparation

The mineral salt medium (MSM) at pH ≈7 was made up according to the method provided (Tendenedzai et al., 2021). All chemicals were sourced from Merck. The MSM was also sterilised via autoclaving at 121 °C for 15 min.

2.3. Gold (iii) stock solution preparation

The chemicals used were ordered from Sigma-Aldrich, Merck unless otherwise specified. To assess the bioreduction ability, gold ion in the form of chloroauric acid ($HAuCl_4{\cdot}3H_2O$) which contains gold (III) ion was used. This was dissolved in deionised water to create a solution containing Au^{3+}/ Au (III) ions. The solid gold (III) chloride ($HAuCl_4{\cdot}3H_2O$) was dissolved in distilled water to create a stock solution of 316.3 ppm Au^{3+} as measured by the Atomic Absorption Spectrometer (AAS). The pH was adjusted to 7 to neutralise the acidic nature of $HAuCl_4$ and make it conducive for the bacteria using 0.01 M HNO_3 or 0.01 M NaOH, accordingly. The stock solution was kept in an amber bottle in a cold room to avoid degradation.

2.4. Sampling and source of microorganism

Samples of the gold tailings and mine wastewater were taken as grab samples from various spots (including old dumps and newly processed dumps of tailings) at a small scale mine in Chinhoyi, Zimbabwe and stored in a cooler box at 4 ℃. These samples were the sources of all the microorganisms used in this study.

2.5. Microbial isolation, adaptation, storage and bacterial analysis

Bacteria were isolated from various gold mine tailings and wastewater samples, representing naturally occurring strains in these environments. To select Au(III)-tolerant bacteria, 0.5 g of each sample (stored at 4 °C) was inoculated into 150 mL of sterile nutrient broth (Tryptone Soy Broth, TSB) amended with 2 mL of Au (III) solution 10 ppm (as chloroauric acid), and incubated (35 ± 2 °C, 120 rpm, 24 h) in a shaking incubator, Scientific Labex Model 353. Following incubation, cultures were streaked onto agar plates some plain and others laced with Au (III) and incubated overnight at 35 °C. Only bacteria that grew in both the gold-laced broth and on gold-containing agar were selected for further experiments. These strains were considered adapted, having been acclimatised to the presence of Au (III), and tolerant to the harsh chemical conditions typically associated with mining environments, such as high sulfur and cyanide levels (Mpeta et al., 2025).

The characterization and identification of the bacteria was performed using 16S rRNA gene sequencing, from a third-party laboratory, Inqaba Biotechnical Industries (Pty) Ltd. (Pretoria, South Africa). Genomic DNA was extracted from the cultures received using the Quick-

DNATM Fungal/Bacterial Miniprep Kit (Zymo Research, Catalogue No. D6005). The primers used were 16S-27F (AGAGTTTGATCMTGGCTCAG) and 16S-1492R (CGGTTACCTTGTTACGACTT). More details on the methods are provided in the supplementary material, Table S1. The bacteria were also stored under glycerol and stored in the −76 °C freezer, for future use.

2.6. Growth experiments and NADH measurement

Based on the results of the previous experiments, growth conditions were set at pH 7 ± 0.5 and temperature range of 35–40 °C for all bacteria. This is because all the 4 strains of bacteria have the same optimum pH range and temperature range according to literature (Kebabcı & Cihangir, 2011; Mahdi et al., 2014; Tunçel & Göktan, 1990). The isolated bacteria were inoculated in 150 mL of broth prepared as outlined in section 2.1 at pH7 ± 0.5 and incubated in a shaking incubator (Scientific Labex Model 353) at 120 rpm and 35 ± 2 °C. The optical density (OD) of the bacterial culture measured at a wavelength of 600 nm (OD 600) was used to estimate the concentration of bacterial cells in a liquid culture. Periodic samples were taken and OD600 measured using a PerkinElmer Lambda 950 UV–VIS spectrophotometer (dual-beam technology). In addition to the OD600, pH and oxidation- reduction potential (ORP) were measured using measuring probes (PL700AL, Pacific Sensor Technologies, Neutron Place Rowville, Victoria, Australia). For NADH, UV–VIS spectroscopy was used where the optical density at 340 nm was used to indicate the presence of the reducing agents, NADH (reduced Nicotinamide adenine dinucleotide).

2.7. Gold bioreduction batch experiments

Amber plastic bottles (250 mL volume) were acid washed, rinsed and air-dried overnight in preparation for the gold reduction experiments. The gold stock solution in the form $HAuCl_4{\cdot}3H_2O$ was added to the MSM (described in section 2.2) giving a starting concentration of 6 ppm and 3 ppm for the reduction experiments.

Triplicate reactors were set up with prepare Au (III)- MSM at a pH of 7. The different bacterial strains grown in broth for 24 h to reach stationary phase were centrifuged to give a concentrated pellet which was used for the reduction experiments. Each triplicate set was inoculated with the different strain of *B. cereus*, *S. maltophilia*, *A. bereziniae*, *K. pneumoniae* and the consortium respectively. Negative control with gold solution without bacteria was set up to check abiotic reduction and a positive control with bacteria without gold to assess any background gold contamination was also set up. The reactors were placed in an incubator at a temperature of 35 ± 2°C on a shaking table set at 120 rpm for 24 h. Samples were taken periodically and centrifuged. The supernatant was taken for AAS analysis. The residue was stored in the freezer for further analysis. All experiments were performed in triplicate (n = 3), with error bars in the results indicating standard deviation, unless specifically noted otherwise.

2.8. Gold (III) and glucose measurements

The Au (III) concentrations were determined using an Atomic Absorption Spectrophotometer (Perkin Elmer A Analyst, Model AA400, CA, USA) at 242.8 nm wavelength equipped with a 290 mA gold lamp. The equipment was calibrated using gold (III) standard solution at 1, 2, 5 and 10 ppm. A sample of approximately 7 mL was drawn at each sampling time, centrifuged and the supernatant taken for Au (III) analysis.

Residual glucose in the supernatant was done using CONTOUR®PLUS blood glucose monitoring system (CP BGMS, Bayer, Ascensia Diabetes Care, Basel, Switzerland). This was accurate as supported by other studies which proved that the CP BGMS had a lower mean difference from the reference value than other systems across various glucose ranges (Dunne et al., 2015).

2.9. Structural and compositional characterization techniques

2.9.1. SEM sample preparation and analysis

The bacterial cultures grown in the absence of gold and in the presence of 0.5 mM Au (III) were collected after 24 h of incubation at 35 ± 2 °C. The cells were harvested using centrifugation (6000 rpm, 5 min) and fixed with 2.5 % glutaraldehyde in 1.5 M phosphate buffer for 30 min. The cells then underwent post-fixation treatment in 1 % osmium tetroxide (OsO_4) for 30 min. The samples were dehydrated with alcohol after which they were processed using standard procedures for SEM and mounted on copper grids (Tendenedzai et al., 2021). The analysis was conducted by scanning electron microscope (SEM) FEGSEM: Zeiss 540 Ultra.

2.9.2. X- ray diffraction (XRD) and X-ray photoelectron spectroscopy (XPS)

The crystallinity of the nanoparticles was studied by X-Ray Diffraction (XRD) with an X-ray diffractometer (Rigaku Corporation, Tokyo, Japan). The material was prepared for XRD analysis using a back-loading preparation method. Diffractograms were obtained using a PANalytical X'Pert Pro diffractometer with an X'Celerator detector and variable divergence- and fixed receiving slits with Fe-filtered Co-Kα radiation. The phases were identified using X'Pert Highscore Plus software and PAN-ICSD. The relative phase amounts (weight %) were estimated using the Rietveld method. The prepared nanoparticles were mounted on a stainless steel holder, and the XPS analysis was performed using a high-performance X-ray photoelectron spectrometer (Model Escalab 250Xi; Thermo Scientific Co.,Waltham, MA, USA) with monochromatic Al Kα radiation of energy 1,486.6 eV. Method is detailed in supplementary Fig. S3.

3. Results and discussions

The microbial reduction of Au (III) to Au (0) plays a crucial role in mimicking conditions found in tailings and low-grade ore environments, where bacteria could potentially catalyze gold reduction processes. To investigate the microbial mechanisms bacterial strains were exposed to gold (III) ion concentrations of 3 ppm and 6 ppm, which represent typical levels found in tailings (Ubaldini et al., 2019).

3.1. Microbial characterization

The characterization of the bacterial strains was conducted on colonies that had been grown on gold laced agar. Characterization done by Inqaba Biotechnical Industries Private Limited gave the photographic image of the 16S target region, BLAST results and 16S report (provided as supplementary material, Table S1). The bacteria strains were identified as *Klebsiella pneumoniae* (*K. pneumoniae* or KP), *Acinetobacter bereziniae* (*A. bereziniae* or AB) and *Strenophomonas maltophilia* (*S. maltophilia*, or SM), and *Bacillus cereus*, *B. cereus* or BC). These four strains were combined to form a mixed consortium.

The four were combined as some studies have indicated that the use of a consortium may give better reduction rates in bioremediation, as in the study on bioremediation of heavy metals (Singh & Vaishya, 2017). Additionally, bacterial strains are likely to coexist in the same environments as consortia as opposed to individual strains.

3.2. Minimum inhibitory concentration and bacterial growth in the presence of Au (III)

3.2.1. Minimum inhibitory concentration

The bacterial strains were streaked on agar plates laced with Au (III) at various concentrations (20 ppm, 50 ppm, 100 ppm, and 200 ppm) as shown in figure 1 to assess their tolerance to Au (III) ions, a critical factor in evaluating their suitability for bioreduction processes. This approach allowed for the determination of the minimum inhibitory concentration

(MIC), defined as the lowest concentration of Au (III) that completely inhibits bacterial growth. Gold (III) was incorporated into the agar as chloroauric acid ($HAuCl_4 \cdot 3H_2O$), and the growth of bacterial colonies was monitored to gauge their resilience to metal toxicity, as illustrated in Fig. 1 for *Bacillus cereus*.

While the research focused on lower Au (III) concentrations (3–6 ppm), typical of gold tailings and wastewater, determining the MIC at higher concentrations was essential to identify robust bacterial strains capable of withstanding the harsh chemical environments of gold mining effluents, which often contain elevated levels of heavy metals and other toxicants like cyanide. The results showed that all tested strains, *Klebsiella pneumoniae, Acinetobacter bereziniae, Stenotrophomonas maltophilia,* and *Bacillus cereus*, formed fewer colonies as Au (III) concentrations increased, with sparse growth observed at 200 ppm and no growth above this threshold, establishing 200 ppm as the MIC. This trend, consistent across all strains, highlights their adaptive capacity to tolerate Au (III) toxicity, likely due to mechanisms such as efflux pumps, enzymatic detoxification, or biosorption, which are critical for their survival in metal-rich environments (Tendenedzai et al., 2021). Although Fig. 1 specifically depicts B. *cereus*, the similar trend across all strains underscores their shared resilience, with gram-negative bacteria potentially benefiting from outer membrane-mediated resistance mechanisms.

Further to this, more quantitative experiments were done in batch reactors at different gold concentrations (0 ppm, 20 ppm, 50 ppm, 100 ppm, 200 ppm and 300 ppm) to determine the minimum tolerable concentration of Au (III) by different bacterial strains and results were displayed in Fig. 2. Without any Au (III) added to the growth media, all bacteria strains exhibited OD 600 above 4. As the Au (III) was introduced, at 20 ppm, the OD 600 was reduced in the three bacteria except for *A. bereziniae*. This might have been due to the stress response of that particular strain (Sanyal et al., 2023).

From 20 ppm – 100 ppm, the maximum growth reached per strain reduced drastically. At 200 ppm the maximum growth of the bacteria was very low but slightly higher than the starting value of OD 600 confirming this as the MIC. At 300 ppm, the OD 600 was lower than the values at t_0. Identifying the MIC not only confirms the strains' robustness for biocatalytic applications but also provides insights into their potential for industrial-scale bioremediation and gold nanoparticle synthesis, where tolerance to fluctuating metal concentrations is crucial for process stability and efficiency.

3.2.2. Bacterial growth in the presence of Au (III)

After culturing the bacteria for 24 h in broth as explained in section 2.6, the growth rate for the four strains and the consortium were plotted as shown in Fig. 3.

During the initial 0–5 h period, bacterial growth, as measured by optical density (OD600), was slow for all individual strains (*Klebsiella pneumoniae, Acinetobacter bereziniae*, *Stenotrophomonas maltophilia*, and *Bacillus cereus*), reflecting their adaptation to the Au (III)-laced environment. This lag phase is likely due to the bacteria adjusting to the presence of toxic Au (III) ions, which can disrupt cellular processes by inducing oxidative stress or interfering with membrane integrity. In contrast, the microbial consortium exhibited significantly higher growth during this period compared to the individual strains. This enhanced

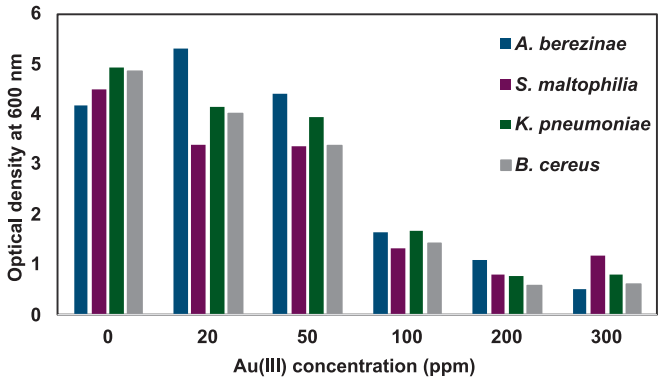

Fig. 2. Optical density at 600 nm, an indication of bacterial growth at different Au (III) concentrations in 24 h.

growth can be attributed to the synergistic interactions among the diverse species, which possess complementary metabolic pathways. For instance, the consortium likely benefited from resource partitioning, where fast-growing opportunists like *K. pneumoniae* and *A. bereziniae* efficiently utilized glucose, while *S. maltophilia* and *B. cereus* contributed secondary metabolites or extracellular enzymes that facilitated detoxification of Au (III). These interactions enabled the consortium to adapt more rapidly to the metal-stressed environment, supporting higher biomass production and setting the stage for efficient Au (III) bioreduction.(Otwell et al., 2018; Sitnikova et al., 2022).

Between 5–10 h, all bacterial strains exhibited exponential growth, as measured by OD600, with *Acinetobacter bereziniae* and *Klebsiella pneumoniae* showing the most significant increases after 8 h. During this phase, the consortium's growth surpassed that of *Stenotrophomonas maltophilia* and *Bacillus cereus* but was lower than *A. bereziniae* and *K. pneumoniae*. After 8 h, the consortium maintained higher viable cell counts, while *S. maltophilia* and *B. cereus* monocultures declined, likely due to metal-induced stress. *S. maltophilia*, adapted to nutrient-poor environments with a doubling time of 2–4 h (Lahiri et al., 2021; Ryan et al., 2009), and *B. cereus*, with a faster doubling time of 20–30 min but prone to stress-induced sporulation (Lao et al., 2020; Vilain et al., 2006), were less resilient. In contrast, the fast-growing *A. bereziniae* and *K. pneumoniae* (doubling times ~ 20–40 min) (Sitnikova et al., 2022) likely enhanced the consortium's adaptability, sustaining growth and facilitating early Au (III) reduction through synergistic metabolic interactions.

Between 10—22 h, there is slow growth for all strains. In the gold laced environment, all strains do not have a prolonged stationary phase as they do in the gold free environment. This measurement of growth in gold laced broth helped to reflect successful growth despite gold presence hence helped predict the sustainability of the biocatalytic process and the potential for continuous gold reduction in industrial applications. (Yougbare et al., 2019; Zheng et al., 2017).

3.3. Au (III) bio-reduction for the different bacterial strains

Samples from the reactors were centrifuged, and the supernatant was analyzed for Au (III) concentrations using Atomic Absorption

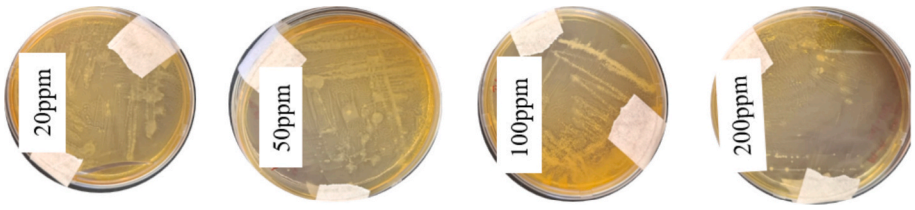

Fig. 1. Growth of *B. cereus* on agar plates with increasing concentration of Au (III) at 20 ppm, 50 ppm, 100 ppm to 200 ppm.

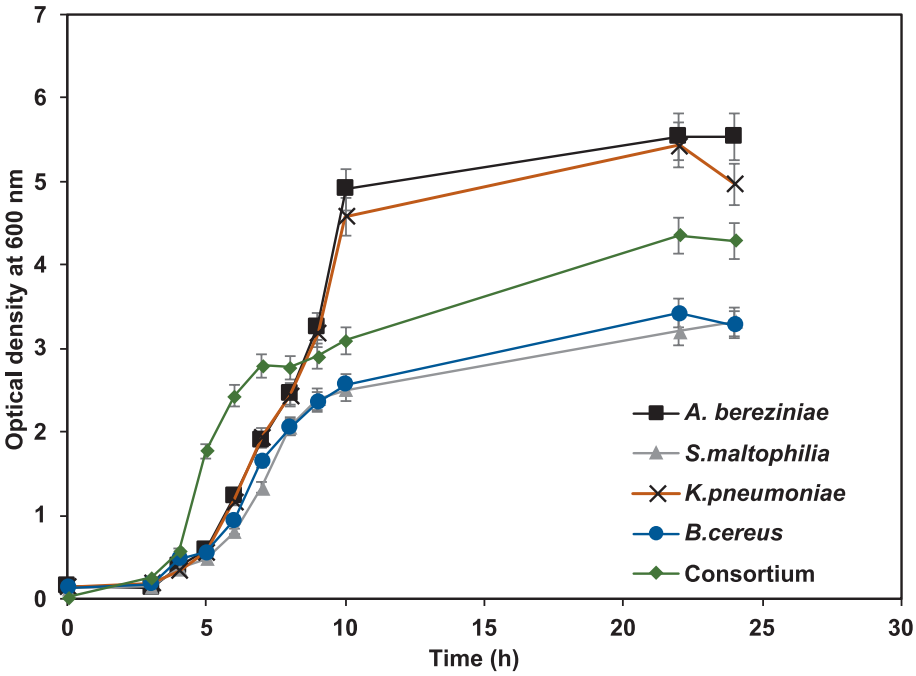

Fig. 3. OD600 for individual strains and consortium in broth within 24 h in the presence of Au (III) at 6 ppm.

Spectroscopy (AAS) at 242.8 nm. A visible color change in the reaction mixture, from yellow to pinkish-red or dark blue purple (Fig. 4), indicated the initial formation of gold nanoparticles (AuNPs). This color shift, driven by the surface plasmon resonance of Au (0), confirmed the bioreduction of Au (III) to elemental gold. (Wang et al., 2022b).

After 12 h of reduction experiment, visible precipitates formed in the reactors, transitioning from the initial yellow mixture to red or dark blue- purple, as shown in Fig. 4. These color variations, attributed to surface plasmon resonance of Au (0) nanoparticles, suggest differences in AuNP size and morphology, consistent with previous studies (He et al., 2005; Jain et al., 2006; Lee et al., 2020), reflecting the influence of bacterial bioreduction mechanisms.

Bacterial growth (OD600) followed similar trends at 3 mg/L and 6 mg/L Au (III) concentrations as shown in figure 5 a-e. The control experiment, without bacteria, showed minimal Au (III) reduction (<1.5 % over 24 h), confirming that reduction was primarily driven by bacterial activity and their metabolites (Duman & Akda, 2024; Iravani, 2014; Wang et al., 2020). At 6 mg/L, all strains achieved faster reduction (>75 % within 4 h) compared to 3 mg/L (<50 %), likely due to chemical kinetics, where higher substrate concentrations enhance reaction rates, as described by the Michaelis-Menten model for enzyme-mediated processes (J. Li et al., 2016; Segel, 1993). Additionally, elevated Au (III) levels may trigger stress responses, prompting bacteria to upregulate reductive enzymes to detoxify the toxic ions (Tendenedzai et al., 2021). While all strains reduced Au (III), the extent of reduction varied, reflecting differences in their metabolic and enzymatic capacities.

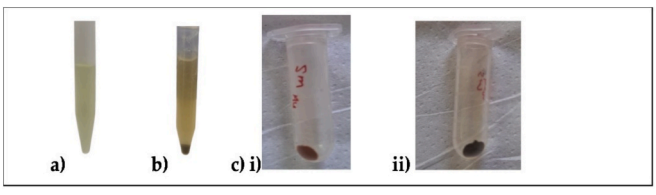

Fig. 4. Color change within the first 12 h of Au (III) reduction: a) before reduction; b) after reduction, c) after reduction and centrifuging (i) red, ii) dark blue). (For interpretation of the references to colour in this figure legend, the reader is referred to the web version of this article.)

3.3.1. Au (III) reduction by A. bereziniae, K. pneumoniae and S. maltophilia (gram negative strains)

During the initial 4 h, *Acinetobacter bereziniae, Klebsiella pneumoniae,* and *Stenotrophomonas maltophilia* (Fig. 5b; d and e), exhibited pronounced Au (III) reduction despite minimal growth (OD600), driven by stress response mechanisms. Toxic Au (III) ions, which disrupt cell membranes and cellular processes, likely triggered rapid detoxification via upregulated metal resistance genes and reductase enzymes (Duman & Akda, 2024; Wang et al., 2020). Pre-existing extracellular polymeric substances (EPS) and constitutively expressed membrane-bound reductases facilitated reduction without significant proliferation (Kang et al., 2017; Wang et al., 2022). By prioritizing detoxification over-growth, bacteria diverted energy to reduction mechanisms, explaining the inverse relationship between Au (III) reduction and cell division in this early phase (Cui et al., 2012).

Between 4–12 h, progressive Au (III) reduction coincided with increased bacterial growth (OD600), indicating a link between bioreduction and microbial metabolic activity. Bacteria likely utilized Au (III) as an electron acceptor during respiration, generating energy to support cellular processes (Reith et al., 2006). Additionally, reducing toxic Au (III) to elemental Au (0) alleviated cellular stress, further promoting growth by minimizing membrane disruption and oxidative damage (Reith et al., 2006; Wang et al., 2020).

After 12 h, bacterial growth (OD600) entered the stationary phase with minimal increases, likely due to nutrient depletion driven by high metabolic activity during Au (III) reduction. The bioreduction process yielded elemental Au (0) nanoparticles, confirmed by SEM, EDS, and XRD. These nanoparticles may adsorb onto bacterial cell surfaces, potentially disrupting nutrient uptake and membrane integrity, further contributing to reduced growth rates (Das et al., 2009; Paesa et al., 2023).

The overall gold reduction by 3 strains was between 98.33 %-99.8 % in 24 h. Of the bacterial strains investigated, all Gram-negative strains are recognized for their robust resistance to heavy metals and antibiotics, underpinning their efficacy in bioremediation and catalytic applications (Desouky, 2003; Maeda & Tsuruta, 2020; Pineda et al., 2023). These microorganisms exhibit capacity to detoxify heavy metals, such as Au (III), through bioreduction, facilitating the synthesis of catalytically active gold nanoparticles (Reith et al., 2006). Their outer membrane

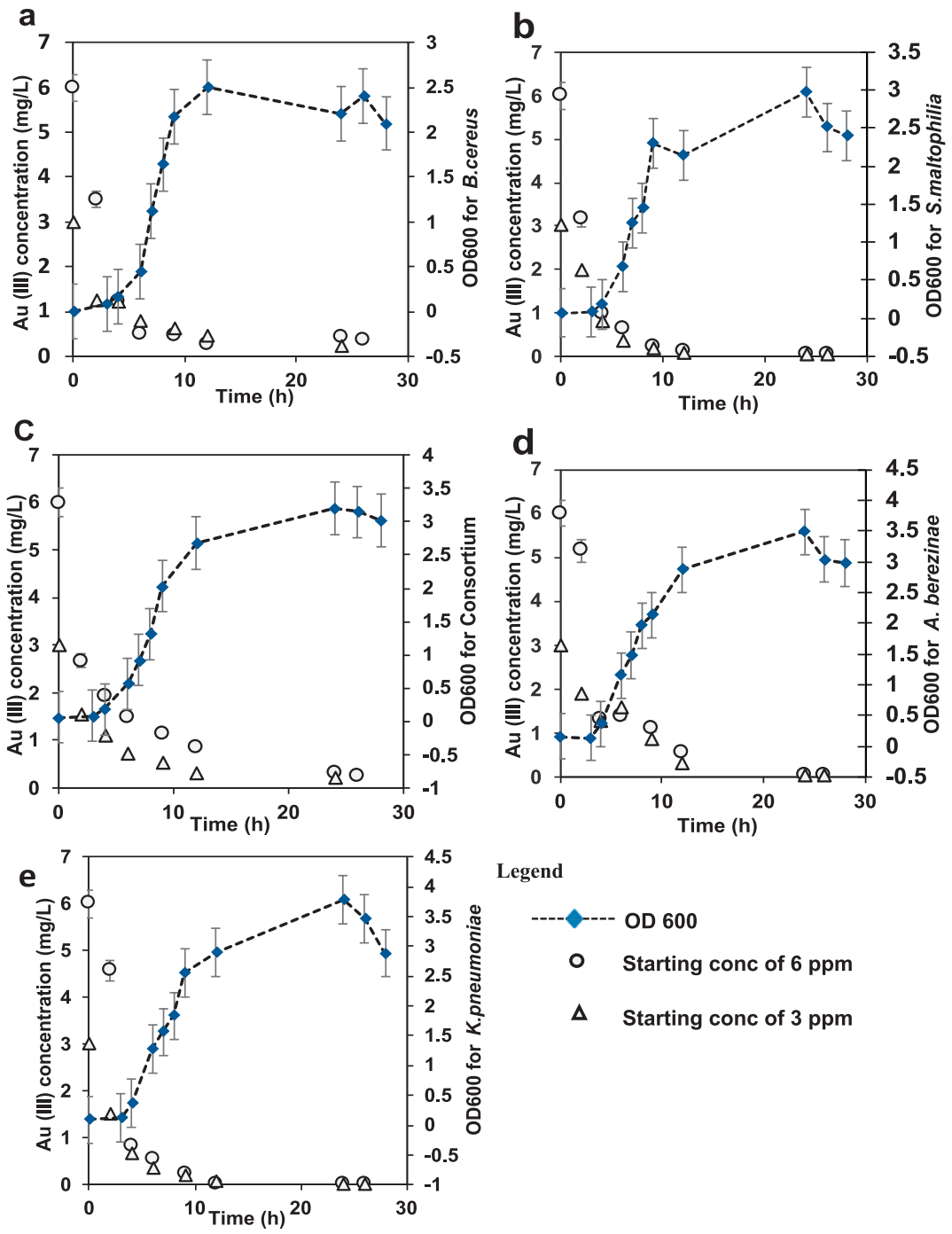

Fig. 5. Au (III) bio- reduction over 24 h period from 3 mg/L and 6 mg/L and OD600 at 6 mg/L by a) *B. cereus*, b) *S. maltophilia*, c) Consortium, d) *A. bereziniae* and e) *K. pneumoniae.*

structure and associated resistance mechanisms enhance their potential for sustainable metal recovery and green catalysis, positioning them as promising agents for environmentally friendly catalytic processes such as biodegradation, leaching, and the production of important bio-products (Desouky, 2003; Pande et al., 2022). Though they have not been extensively used for Au (III) reduction compared to other bacteria (such as *Pseudomonas* or *Bacillus* spp.), these species are known for biosorption of heavy metals via cell wall components such as lipopoly-saccharides and membrane proteins. Au (III) could initially bind to the cell surface, followed by reduction to Au (0), forming nanoparticles either extracellularly or intracellularly (Panda and Deepa, 2011). Au (III) reduction is likely mediated by reductase enzymes, similar to those involved in Cr (VI) reduction (Montes-Robledo et al., 2024).

3.3.2. Au (III) reduction by gram positive B. cereus

From figure 5a, the first 4 h, *Bacillus cereus* reduced Au (III) by 59–78 %, the lowest among the four strains, despite slightly higher growth (OD600) compared to Gram-negative bacteria. This lower efficiency may result from the thick peptidoglycan layer of Gram-positive bacteria, which likely hinders Au (III) uptake and metabolic interactions compared to the outer membrane-mediated resistance mechanisms of Gram-negative strains (Maeda & Tsuruta, 2020; Reith et al., 2006).

Between 4–12 h, *Bacillus cereus* exhibited exponential growth (OD600), similar to Gram-negative strains, as Au (III) concentrations

decreased. The stationary phase occurred from 12–24 h, likely due to nutrient depletion from the high metabolic demands of Au (III) reduction. After 24 h, *B. cereus* achieved a reduction in efficiency of 92.9 %, the lowest among the strains. As the only Gram-positive bacterium, *B. cereus* likely reduces Au (III) to Au (0) via NADH-dependent reductases (reduced Nicotinamide Adenine Dinucleotide, NADH) and extracellular metabolites, with biosorption on its peptidoglycan-rich cell wall initiating the process (Lin et al., 2011; Wang et al., 2022). Its facultative metabolism and spore-forming ability enhance its versatility for Au (III) reduction (Abee et al., 2011; Bottone, 2010; Lao et al., 2020).

3.3.3. *Au (III) reduction efficiency by consortium against individual strains*

The consortium (figure 5c) was comprised of all the 4 bacteria strains under investigation. During the initial 4 h period, the consortium exhibited higher growth than all the other individual strains. This is likely due to synergistic metabolic interactions and enhanced heavy metal resistance (Desouky, 2003; Pande et al., 2022). Complementary nutrient utilization and efficient electron transfer within the consortium optimized energy acquisition, supporting growth and biomass production while facilitating the synthesis of catalytically active Au (0) nanoparticles (Reith et al., 2006).

Between 4 and 12 h of Au (III) bio-reduction, the microbial consortium likely achieved more efficient and stable formation of Au (0) nanoparticles, as shown in the graph. This may be ascribed to collaborative enzymatic activities and extracellular matrix stabilization (Khidr et al., 2025; Reith et al., 2006). These nanoparticles, exhibiting potential catalytic activity, may have diminished Au (III) toxicity by seizing the metal ions, thereby fostering a less stressful environment conducive to enhanced microbial growth (Reith et al., 2007). This dynamic is particularly significant, as the consortium closely mimics the microbial diversity and interactions found in natural gold tailings environments, enhancing its relevance for in situ bioremediation and sustainable catalysis (Desouky, 2003; Li et al., 2011; Pineda et al., 2023).

The reduction efficiency of the four individual strains of bacteria was compared to the consortium at 6 ppm of Au (III). The gold (III) reduction efficiency was calculated as:

$$\textbf{Reduction efficiency, } \mathbf{R} = \frac{\mathbf{C_{O,\,Au(III)}} - \mathbf{C_{e,\,Au(III)}}}{\mathbf{C_{O,\,Au(III)}}} \quad (1)$$

where $C_{O,\,Au\,(III)}$ −Initial Au (III) Concentration
$C_{e,\,Au\,(III)}$- Final Au (III) Concentration

Within the first 4 h, all gram- negative bacteria achieved higher reduction efficiencies (75–80 %) while the consortium (70–75 %) achieved a higher reduction than *B. cereus* (59–65 %) as illustrated in Fig. 6.

The microbial consortium, comprising three gram-negative bacteria and one gram-positive, outperformed *B. cereus* alone in Au (III) bioreduction, due to the superior reduction capabilities of its Gram-negative constituents (Wang et al., 2020). Notably, *K. pneumoniae* facilitated efficient electron transfer to Au (III) ions even under the aerobic conditions of these experiments, suggesting its versatile respiratory capabilities. While primarily an aerobic process, the microenvironments within bacterial aggregates likely experienced localized oxygen depletion, triggering *K. pneumonia*'s facultative anaerobic metabolism(Wessel et al., 2014). The resultant fermentative byproducts could serve as electron donors for co-occurring species, enhancing synergistic reduction (Li et al., 2013; Malarkodi et al., 2013).

Although the consortium achieved a reduction efficiency of 94.5 % after 24 h, it did not match the 99 % efficiency of individual Gram-negative strains, likely due to the lower reductive capacity of *B. cereus*. Nevertheless, *B. cereus* possibly contributed extracellular enzymes, such as NADH-dependent reductases and thiol-rich peptides, which supported Au (III) reduction under aerobic conditions, complementing the consortium's versatility (Thirumurugan et al., 2012). The resulting Au (0) nanoparticles, confirmed by microscopy, underscore the consortium's potential for sustainable metal recovery and green catalysis, with Gram-negative bacteria demonstrating greater reduction potential than their Gram-positive counterpart (Khidr et al., 2025; Modestra & Mohan, 2014; Reith et al., 2006).

3.4. *Possible Au reduction mechanism in the cell structure*

The bioreduction process from Au (III) to Au (0) requires electrons that the system provides using various ways. NADH serves as the electron donor and Au (III) as the electron acceptor, resulting in the reduction of Au (III) to metallic Au (0) while NADH is oxidized to NAD^+ ($C_{21}H_{27}N_7O_{14}P_2$).

$$Au^{3+} + 3e^- \rightarrow Au^0 \quad (2)$$

Primarily, enzymes such as NADH-dependent reductases use NADH ($C_{21}H_{29}N_7O_{14}P_2$) or NADPH (reduced Nicotinamide Adenine Dinucleotide Phosphate, $C_{21}H_{30}N_7O_{17}P_3$) as electron donors. The oxidation of NADH provides electrons:

$$NADH \rightarrow NAD^+ + H^+ + 2e^- \quad (3)$$

For reduction of Au (III), electrons from NADH reduce Au (III):

$$3NADH + 2Au^{3+} \rightarrow 3NAD^+ + 3H^+ + 2Au \quad (4)$$

In a same way, NADPH oxidation also provides electrons:

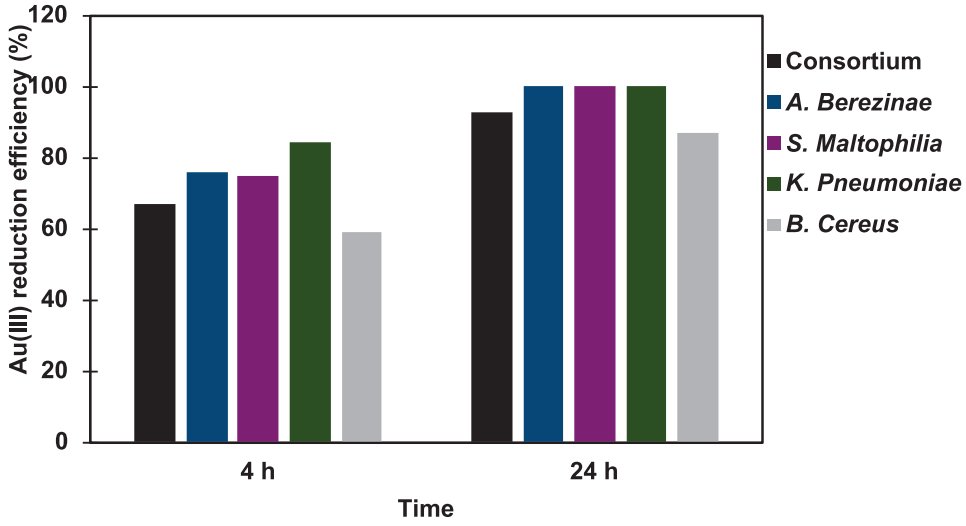

Fig. 6. Comparison of Au (III) percentage reduction between consortium and individual strains over 4 h and over 24 h.

$$3NADPH + Au^{3+} \rightarrow 3NADP^{+} + 3H^{+} + Au \quad (5)$$

Biomolecules can serve as electron donors including thiols (R-SH), phenols, or amines in proteins. The thiol group in protein or glutathione may oxidize as follows:

$$2R - SH \rightarrow R - S - S - R + 2H^{+} + 2e^{-} \quad (6)$$

These electrons reduce Au (III), giving the overall reaction as:

$$Au^{3+} + 3R - SH \rightarrow Au + 1.5R - S - S - R + 3H^{+} \quad (7)$$

3.4.1. NADH consumption versus Au (III) concentration

The reduction process was monitored through the UV–Vis spectroscopy technique, as the optical density (OD) at 340 nm can be used to indicate the presence of reducing agent, NADH (Krysiuk, 2020). NADH absorbs strongly at 340 nm, and these measurements are commonly used to quantify its concentration, which can indicate the activity of NADH-dependent enzymes involved in bioreduction of gold (Huang et al., 2005).

All four bacterial strains tested at pH 7, 35 °C with controls of abiotic Au (III) were used for background absorbance corrections. There was consumption of NADH during Au (III) bioreduction, as evidenced by decreasing OD 340 (Fig. 7) with increasing Au (III) concentration after 24 h. This aligns with the referenced study's findings that NADH is a key electron donor in Au (III) reduction to AuNPs (Huang et al., 2005; Krysiuk, 2020).

K. pneumoniae, A. bereziniae and *S. maltophilia* used in this study are gram- negative bacteria. (Abee et al., 2011) occurs across the outer membrane, periplasm, and cytoplasm, facilitated by a continuous electron transfer pathway mediated by cytochromes located in these cellular compartments (Li et al., 2013; Maeda & Tsuruta, 2020). These bacteria leverage outer membrane proteins for biosorption and enzymatic reduction, periplasmic cytochromes for electron transfer, and intracellular enzymes for cytoplasmic reduction, leading to the formation of catalytically active Au (0) nanoparticles (Campaña et al., 2023; Desouky, 2003; Lin et al., 2011).

Conversely, *Bacillus cereus*, the only Gram-positive bacterium in the study, lacks an outer membrane and has a reduced periplasmic space, which likely constrains its reductive capacity (Bottone, 2010; Nielsen & Lampen, 1982; Pourali et al., 2017). Although its thick peptidoglycan layer can adsorb and reduce Au (III) through interactions with biopolymers, this process is less efficient due to reduced ion accessibility and limited extracellular reductive mechanisms (Li et al., 2016; Li et al., 2011; Pourali et al., 2017). The interaction of Au (III) with oxygen- and nitrogen-containing groups in cell wall polysaccharides and proteins, particularly in Gram-negative bacteria, induces changes that enhance binding to peptide bonds and side chains, further promoting reduction (Lin et al., 2011). These mechanistic differences account for the superior reduction efficiency of Gram-negative strains (approximately 99 %) compared to *B. cereus* (92.9 %), underscoring their potential for sustainable metal recovery and green catalysis in mining effluent treatment (Reith et al., 2006). This efficiency is driven by distinct bioreduction pathways, which vary between Gram-negative and Gram-positive bacteria.

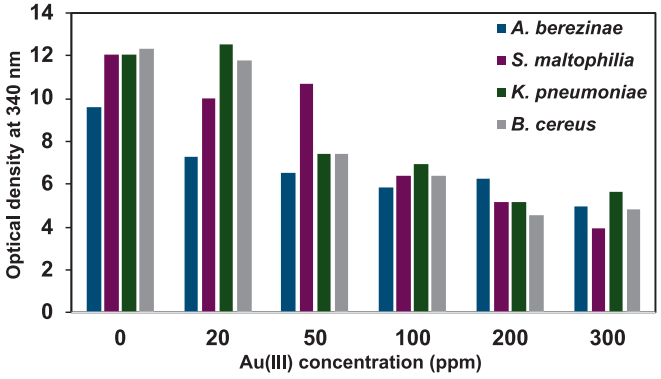

Fig. 7. Optical density at 340 nm as an indication of NADH for the four bacterial strains in 24 h.

While the NADH consumption assays provide supportive evidence for the involvement of NADH-dependent reductases in Au (III) reduction, they were conducted primarily to indicate electron donor utilisation and were not designed to yield detailed kinetic parameters or identify specific enzymes. Enzyme activities were not quantified in units of specific activity, and the assays were performed under neutral pH in synthetic Au (III) solutions without accounting for the influence of other environmental factors such as acidity, salinity, or competing ions.

Building on these differences, the biosynthesis of gold nanoparticles occurs through multiple mechanisms, including extracellular reduction by exopolysaccharides(Khan & Ahmad, 2014), cell wall reduction, and intracellular enzymatic processes (Liu et al., 2018) as illustrated by Fig. 8. While Gram-negative bacteria leverage outer membrane and periplasmic cytochromes for efficient reduction, achieving up to 99 % efficiency, *B. cereus* relies on cell wall peptidoglycan and intracellular enzymes, resulting in a lower efficiency of 92.9 %. Notably, the shared intracellular reduction mechanisms across both bacterial types highlight the adaptability of biological systems in producing catalytically active nanoparticles.

3.5. Glucose consumption during Au (III) reduction in 24 h

During gold (III) reduction, the pH and ORP were monitored and remained constant in the range of 7–7.5 (pH) and −110 to −80 mV (ORP) over the 24 h period. The growth medium contained glucose as the primary carbon source at an initial concentration of 10 g/L (as shown in Fig. 9), facilitating microbial metabolic activity and contributing to the biogenic synthesis of Au (0) nanoparticles (Reith et al., 2006).

From 0–2 h, start with most strains actively metabolize glucose, except SM which seemed to be slower. Initially, *K. pneumoniae* rapidly consumed ~ 2 g/L with a sharp decline, while *A. bereziniae* used 3 g/l, *B. cereus* used 1 g/l and *S. maltophilia* used ~ 0.7 g/L gradually, *B. cereus* consumed ~ 1.2 g/L, and the consortium depleted 2.1 g/L due to synergistic activity among the different strains (Maeda & Tsuruta, 2020; Reith et al., 2007). Between 2–4 h, a drastic decrease of 3.3 g/l by *B. cereus* strain and also by the consortium (2.5 g/l) is noticed while *S. maltophilia* continues with a steady consumption of 0.7 g/l. Between 4–12 h, exponential growth and peak Au (III) reduction drove high glucose depletion with *K. pneumoniae*, *A. bereziniae*, and *S. maltophilia* using ~ 3.5 g/L, *B. cereus* ~ 0.7 g/L, and the consortium ~ 2.4 g/L. From 12–24 h, *K. pneumoniae* consumed 1.5 g/l while *A. bereziniae* and *S. maltophilia* 0.5 g/l depleted glucose at the slowest rate due to its preference for alternative substrates such as amino acids, lactate (Tendenedzai et al., 2021). *B. cereus* consumed ~ 0.3 g/L as sporulation reduced demand, and the consortium ~ 0–1.2 g/L, reflecting prior depletion. The consortium's synergistic metabolism, enhanced by *A. bereziniae* byproduct utilization (such as organic acids, alcohols, and amino acids) (He et al., 2005), optimized glucose use. Glucose remained non-limiting, supporting robust bacterial growth and Au (III) reduction over 24 h.

3.6. Nanoparticle formation

Nanoparticles synthesised were analyzed using SEM, EDS, XRD and XPS to confirm and characterize Au (0) nanoparticle formation.

Before Au (III) exposure (Fig. 10a), the cells appeared to have a smooth surface and less aggregated. However, after exposure to Au (III), there were differences observed on the morphology of the bacterial cells including more cell aggregation with rough surfaces than initially, small electron-dense particles (appearing as bright spots) on bacterial surfaces

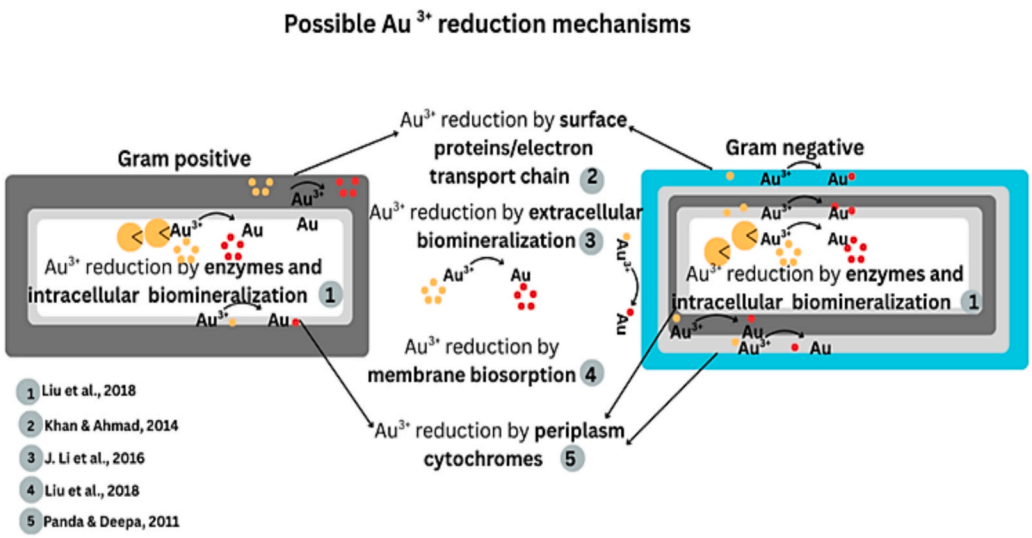

Fig. 8. Possible Au (III) bioreduction mechanisms in gram negative and gram-positive bacteria.

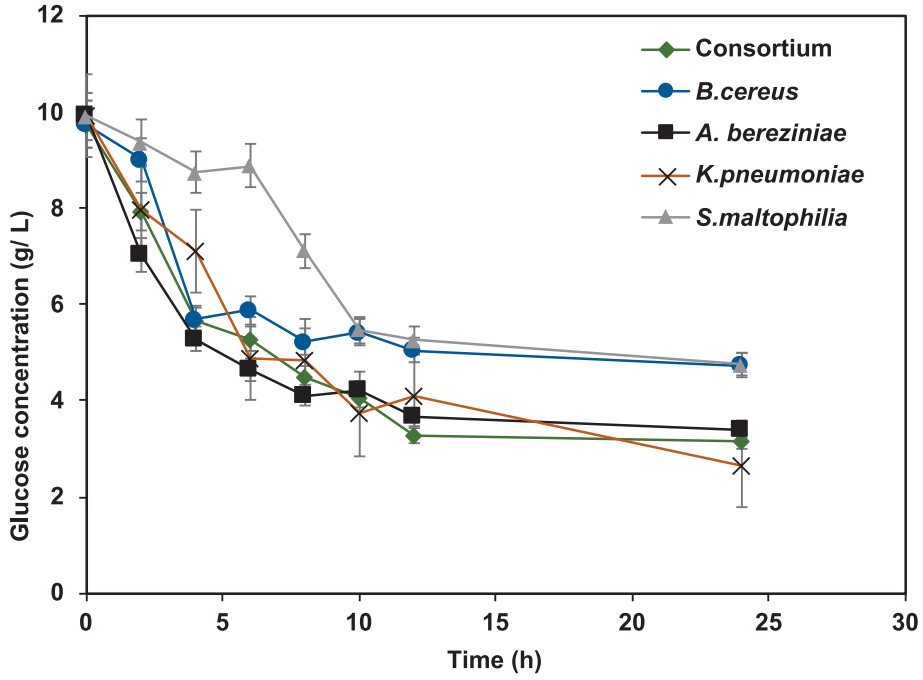

Fig. 9. Glucose depletion during Au (III) reduction (6 ppm) for the four bacterial strains and consortium in 24 h.

and in their vicinity as shown in Fig. 10b. The cells after exposure also appeared noticeably swollen than before exposure. This was a possible stress response during reduction of Au (III) to Au (0) (Wang et al., 2020). Au (III) is toxic to bacteria as it induces bacterial wall damage through electrostatic interactions, promotes reactive oxygen species (ROS) generation, and causes DNA damage (Paesa et al., 2023).

From EDS elemental peaks, Au was identified (Fig. 10c) giving an indication of formation of Au nanoparticles. The EDS spectrum confirms the presence of gold (Au Mα1 peak) in the sample. However, EDS does not tell if crystalline gold was forming to validate successful bio-reduction of Au (III) to elemental gold hence the need for other confirmation tests. The spectrum also indicates the presence of several other elements including sodium (Na), potassium (K), oxygen (O) and other minor elements, which may be from the growth medium and bacterial components. The resulting nanoparticles often have a core–shell structure with a biolayer composed of membrane proteins, lipoproteins, and phospholipids (Liu et al., 2018).

XRD diffractogram from the bacterial cultures after Au (III) reduction identified major phases as halite (NaCl), Sylvine (KCl) and elemental gold (Au). From Fig. 11 (and supplementary S2), the result shows the percentage crystalline content of these constituents after reduction by the consortium: 57.8 % of crystalline content, Sylvine (KCl): 33.7 % of crystalline content and Gold (Au (0)): 8.5 % of crystalline content. The presence of 8.5 % gold in crystalline form is significant evidence of successful bio-reduction. The characteristic gold peaks (likely around 2θ = ~38.2°, ~44.3°, ~64.5°, and ~ 77.6°) are present but relatively small compared to the salt peaks. The 8.5 % gold content is substantial considering that the starting Au (III) concentration was 3–6 ppm, indicating efficient gold reduction and concentration by the bacterial processes.

The XPS spectra in Fig. 11b with the peak for gold (Au) at 84 eV confirmed the presence of Au (0) in gold nanoparticles (AuNPs). The

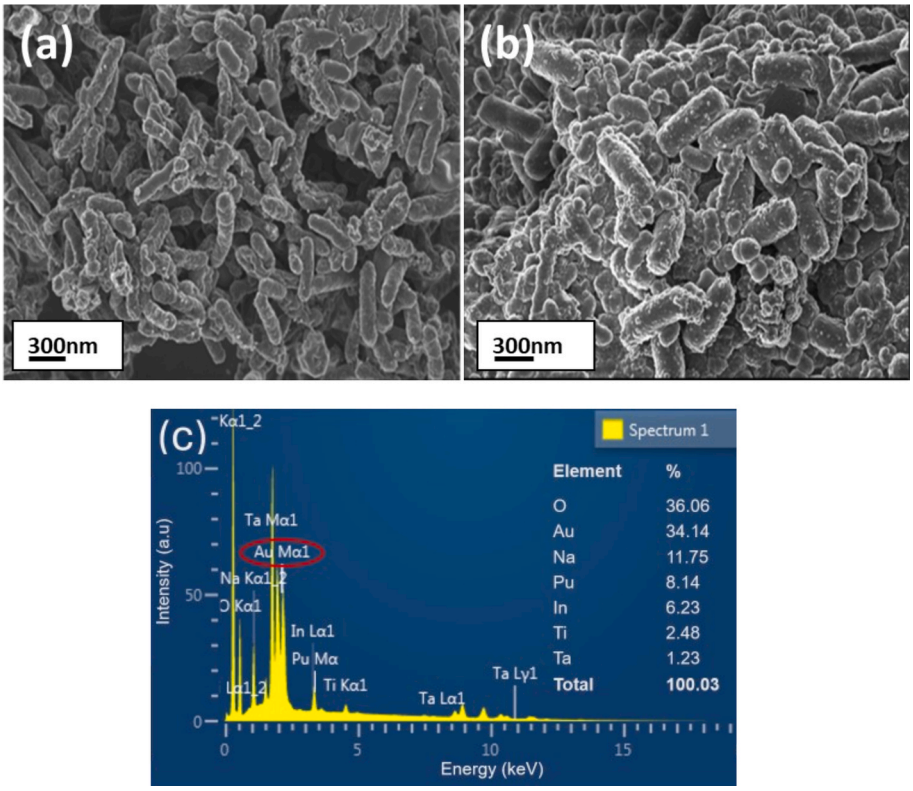

Fig. 10. Images showing a) SEM before exposure for the consortium at 20 000x magnification, b) after exposure to Au (III) at 20 000x magnification and c) EDS showing Au peak after exposure to Au (III).

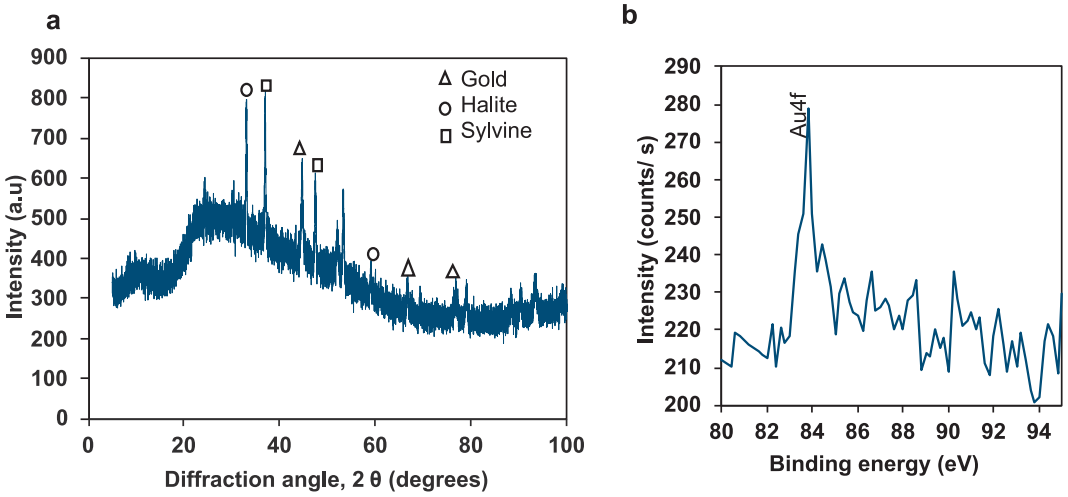

Fig. 11. A) XRD results showing peaks of gold as confirmation of nanoparticle formation by bacterial consortium at 44.3°, ~64.5°, and ~ 77.6°; b) XPS result showing elemental gold Au4f at 84 eV.

peak's low intensity of 275 counts is attributed to the low initial concentration of Au (III) at 6 ppm. Additionally, the bioreduction process results in AuNPs that are heavily coated with biomolecules, which serve as bio- stabilizers(Ahmad et al., 2022). This capping was identified as peaks of carbon, organic nitrogen, organic silica, oxygen and phosphorus.

4. Conclusions

Gram-negative bacteria (*K. pneumoniae*, *A. bereziniae* and *S. maltophilia*) showed higher Au (III) reduction potential than the Gram-positive *B. cereus*. The gram-negative bacteria had a higher Au (III) bioreduction potential (> 99 %) than the gram positive, *B. cereus* 92.9 % which was likely due to the fundamental differences in cell wall structure, membrane transport systems, and extracellular electron transfer mechanisms. The consortium performed better than the *B. cereus* monostrain leveraging on resource partitioning and recycling of metabolites. This showed the importance of having both the gram negative and gram positive being present in the consortium. All strains yielded elemental gold/ Au nanoparticles as identified by the SEM/ EDS, XPS and XRD. The bioreduction of Au (III) by indigenous bacteria and consortia offers a viable, eco-friendly approach to gold recovery, with Gram-negative

bacteria leading in efficiency. Further characterization of the formed gold nanoparticles produced by the different strains is important as this will assist in validating their appropriate applications. Additionally, bioreduction of actual wastewater and metabolomic or transcriptomic analyses are to be explored in greater detail.

CRediT authorship contribution statement

Miranda Mpeta: Writing – review & editing, Writing – original draft, Methodology, Investigation, Formal analysis, Conceptualization. **Job T. Tendenedzai:** Writing – review & editing, Methodology. **Shepherd M. Tichapondwa:** Writing – review & editing, Supervision, Resources. **Evans M.N. Chirwa:** Validation, Supervision, Resources, Funding acquisition, Conceptualization.

Funding

This work is based on research supported in part by the Margaret McNamara Education Grant, the National Research Fund (NRF) through Grant numbers: SRUG2204072544 and CSRP23042396323 awarded to Prof Evans Chirwa and Prof Shepherd Tichapondwa of the Department of Chemical Engineering and auxiliary items financed by the Rand Water Chair in Water Utilization (South Africa).

Declaration of competing interest

The authors declare the following financial interests/personal relationships which may be considered as potential competing interests: Evans M.N Chirwa reports a relationship with Randwater that includes: funding grants. If there are other authors, they declare that they have no known competing financial interests or personal relationships that could have appeared to influence the work reported in this paper.

Appendix A. Supplementary data

Supplementary data to this article can be found online at https://doi.org/10.1016/j.mineng.2025.109797.

Data availability

The data presented in this study are openly available in the University of Pretoria Research Data Repository.

References

Abee, T., Groot, M.N., Tempelaars, M., Zwietering, M., Moezelaar, R., van der Voort, M., 2011. Germination and outgrowth of spores of *Bacillus cereus* group members: Diversity and role of germinant receptors. Food Microbiol. 28 (2), 199–208. https://doi.org/10.1016/j.fm.2010.03.015.

Ahmad, T., Bustam, M.A., Suleman, H., Irfan, M., Iqbal, J., Asghar, H.M.A., 2022. Quantitative Estimation of Biocapped Surface Chemistry Driven Interparticle Interactions and Growth Kinetics of Gold Nanoparticles. J. Clust. Sci. 33 (2), 557–565. https://doi.org/10.1007/s10876-021-01999-5.

Baserisalehi, M., Ahmadi, M., Ghaderinia, P., 2017. Biological Synthesis of Nanoparticles using Bacteria. Journal of Advances in Biology 9 (4), 2027–2032. https://doi.org/10.24297/jab.v9i4.5676.

Bottone, E.J., 2010. *Bacillus cereus*, a volatile human pathogen. Clin. Microbiol. Rev. 23 (2), 382–398. https://doi.org/10.1128/CMR.00073-09.

Campaña, A.L., Saragliadis, A., Mikheenko, P., Linke, D., 2023. Insights into the bacterial synthesis of metal nanoparticles. Front. Nanotechnol. 5 (August), 1–20. https://doi.org/10.3389/fnano.2023.1216921.

Chaturvedi, S., Dave, P.N., Shah, N.K., 2012. Applications of nano-catalyst in new era. J. Saudi Chem. Soc. 16 (3), 307–325. https://doi.org/10.1016/j.jscs.2011.01.015.

Cui, J., Zhang, L., 2008. Metallurgical recovery of metals from electronic waste: a review. J. Hazard. Mater. 158 (2), 228–256. https://doi.org/10.1016/j.jhazmat.2008.02.001.

Cui, Y., Zhao, Y., Tian, Y., Zhang, W., Lü, X., Jiang, X., 2012. The molecular mechanism of action of bactericidal gold nanoparticles on *Escherichia coli*. Biomaterials 33 (7), 2327–2333. https://doi.org/10.1016/j.biomaterials.2011.11.057.

Das, S.K., Das, A.R., Guha, A.K., 2009. Gold nanoparticles: Microbial synthesis and application in water hygiene management. Langmuir 25 (14), 8192–8199. https://doi.org/10.1021/la900585p.

A.-E.-H. Desouky Acinetobacter: environmental and biotechnological applications Afr. J. Biotechnol. 2 4 2003 71–74. www.academicjournals.org/AJB.

Duman, H., Akda, E., 2024. Gold Nanoparticles: Multifunctional Properties, Synthesis, and Future prospects. Nanomaterials 14 (22), 1–56. https://doi.org/10.3390/nano14221805.

Dunne, N., Viggiani, M.T., Pardo, S., Robinson, C., Parkes, J.L., 2015. Accuracy Evaluation of CONTOUR®PLUS Compared with four Blood Glucose monitoring Systems. Diabetes Therapy 6 (3), 377–388. https://doi.org/10.1007/s13300-015-0121-3.

El-Sayed, S., El-Shatoury, E.H., Abdel-Khalek, N.A., Abdel-Motelib, A., Abdel-Khalek, M. A., 2021. Influence of *Bacillus cereus*-gold interaction on bio-flotation of gold in the presence of potassium butyl xanthate. Biointerface Res. Appl. Chem. 11 (5), 13005–13018. https://doi.org/10.33263/BRIAC115.1300513018.

Gardea-Torresdey, J.L., Tiemann, K.J., Gamez, G., Dokken, K., Cano-Aguilera, I., Furenlid, L.R., Renner, M.W., 2000. Reduction and accumulation of gold (III) by *Medicago sativa* alfalfa biomass: X-ray absorption spectroscopy, pH, and temperature dependence. Environ. Sci. Tech. 34 (20), 4392–4396. https://doi.org/10.1021/es991325m.

He, Y.Q., Liu, S.P., Kong, L., Liu, Z.F., 2005. A study on the sizes and concentrations of gold nanoparticles by spectra of absorption, resonance Rayleigh scattering and resonance non-linear scattering. Spectrochimica Acta - Part a: Molecular and Biomolecular Spectroscopy 61 (13–14), 2861–2866. https://doi.org/10.1016/j.saa.2004.10.035.

Huang, X., El-Sayed, I.H., Yi, X., El-Sayed, M.A., 2005. Gold nanoparticles: Catalyst for the oxidation of NADH to NAD+. J. Photochem. Photobiol. B Biol. 81 (2), 76–83. https://doi.org/10.1016/j.jphotobiol.2005.05.010.

Husseiny, M.I., Badr, Y., Mahmoud, M.A., 2007. Biosynthesis of gold nanoparticles using *Pseudomonas aeruginosa*. AIP Conf. Proc. 888, 177–181. https://doi.org/10.1063/1.2711108.

Iravani, S., 2014. Bacteria in Nanoparticle Synthesis: Current Status and Future prospects. International Scholarly Research Notices 2014, 1–18. https://doi.org/10.1155/2014/359316.

Jain, P.K., Lee, K.S., El-Sayed, I.H., El-Sayed, M.A., 2006. Calculated absorption and scattering properties of gold nanoparticles of different size, shape, and composition: applications in biological imaging and biomedicine. J. Phys. Chem. B 110 (14), 7238–7248. https://doi.org/10.1021/jp057170o.

Kang, F., Qu, X., Alvarez, P.J.J., Zhu, D., 2017. Extracellular Saccharide-Mediated Reduction of Au^{3+} to Gold Nanoparticles: New Insights for Heavy Metals Biomineralization on Microbial Surfaces. Environ. Sci. Tech. 51 (5), 2776–2785. https://doi.org/10.1021/acs.est.6b05930.

Kebabcı, Ö., Cihangir, N., 2011. Isolation of protease producing novel *Bacillus cereus* and detection of optimal conditions. Afr. J. Biotechnol. 10 (7), 1160–1164. https://doi.org/10.5897/AJB10.164.

Khan, S.A., Ahmad, A., 2014. Enzyme mediated synthesis of water-dispersible, naturally protein capped, monodispersed gold nanoparticles, their characterization and mechanistic aspects. RSC Adv. 4 (15), 7729–7734. https://doi.org/10.1039/c3ra43888k.

Khidr, R., Qurbani, K., Muhammed, V., Salim, S., Abdulla, S., Wsw, H., 2025. Synergistic effects of indigenous bacterial consortia on heavy metal tolerance and reduction. Environ. Geochem. Health 47 (3), 1–16. https://doi.org/10.1007/s10653-025-02392-1.

Krysiuk, I.P., 2020. The Approach for Express Spectrometric Determination of the Reduced form of Nicotinamide Adenine Dinucleotide (NADH) Content. Biotechnologia Acta 13 (2), 32–37. https://doi.org/10.15407/biotech13.02.032.

Lahiri, D., Nag, M., Sheikh, H.I., Sarkar, T., Edinur, H.A., Pati, S., Ray, R.R., 2021. Microbiologically Synthesized Nanoparticles and their Role in Silencing the Biofilm Signaling Cascade. Front. Microbiol. 12 (February). https://doi.org/10.3389/fmicb.2021.636588.

Lao, C., Shen, Y., Zhu, S., Luo, L., 2020. *Bacillus cereus*, a geobiological marker for gold prospecting isolated from soil from the Jiaodong Gold Mine. J. Geochem. Explor. 215, 106563. https://doi.org/10.1016/j.gexplo.2020.106563.

Lee, K.X., Shameli, K., Yew, Y.P., Teow, S.Y., Jahangirian, H., Rafiee-Moghaddam, R., Webster, T.J., 2020. Recent developments in the facile biosynthesis of gold nanoparticles (AuNPs) and their biomedical applications. Int. J. Nanomed. 15, 275–300. https://doi.org/10.2147/IJN.S233789.

Li, J., Li, Q., Ma, X., Tian, B., Li, T., Yu, J., Dai, S., Weng, Y., Hua, Y., 2016. Biosynthesis of gold nanoparticles by the extreme bacterium *Deinococcus radiodurans* and an evaluation of their antibacterial properties. Int. J. Nanomed. 11, 5931–5944. https://doi.org/10.2147/IJN.S119618.

Li, X., Liu, L., Liu, T., Yuan, T., Zhang, W., Li, F., Zhou, S., Li, Y., 2013. Electron transfer capacity dependence of quinone-mediated Fe (III) reduction and current generation by *Klebsiella pneumoniae* L17. Chemosphere 92 (2), 218–224. https://doi.org/10.1016/j.chemosphere.2013.01.098.

Li, X., Xu, H., Chen, Z.S., Chen, G., 2011. Biosynthesis of nanoparticles by microorganisms and their applications. J. Nanomater. 2011. https://doi.org/10.1155/2011/270974.

Lin, Z., Ye, Y., Li, Q., Xu, Z., Wang, M., 2011. A further insight into the biosorption mechanism of Au (III) by infrared spectrometry. BMC Biotech. 11. https://doi.org/10.1186/1472-6750-11-98.

Liu, W., Wang, L., Wang, J., Du, J., Jing, C., 2018. New insights into microbial-mediated synthesis of Au@biolayer nanoparticles. Environ. Sci. Nano 5 (7), 1757–1763. https://doi.org/10.1039/c8en00104a.

Maeda, I., Tsuruta, T., 2020. Microbial gold biosortion and biomineralization from aqueous $HAuCl_4$ solution. Minerals 10 (3), 1–9. https://doi.org/10.3390/min10030285.

Mahdi, O., Eklund, B., & Fisher, N. (2014). Laboratory culture and maintenance of *Stenotrophomonas maltophilia*. Current Protocols in Microbiology, SUPPL.32. DOI: 10.1002/9780471729259.mc06f01s32.

Malarkodi, C., Rajeshkumar, S., Vanaja, M., Paulkumar, K., Gnanajobitha, G., & Annadurai, G. (2013). Eco-friendly synthesis and characterization of gold nanoparticles using *Klebsiella pneumoniae*. Journal Of Nanostructure in Chemistry (2013) 3(30) 1-7. http://www.jnanochem.com/content/3/1/30.

Modestra, J.A., Mohan, S.V., 2014. Bio-electrocatalyzed electron efflux in Gram positive and Gram negative bacteria: an insight into disparity in electron transfer kinetics. RSC Adv. 4 (64), 34045–34055. https://doi.org/10.1039/c4ra03489a.

Montes-Robledo, A., Baena-Baldiris, D., Baldiris-Avila, R., 2024. Reduction of Cr (VI) by planktonic cells and biofilm of *Acinetobacter* sp. (ADHR1) isolated from electroplating wastewater. Environ. Technol. Innov. 33. https://doi.org/10.1016/j.eti.2023.103521.

Mpeta, M., Tendenedzai, J. T., Tichapondwa, S. M., & Chirwa, E. M. N. (2025). Effect of Cyanide as a Nutrient Source on bacteria, *Bacillus cereus*, for use in Bioleaching of Gold Tailings. Chemical Engineering Transactions, 117(December 2024), 1075–1080. DOI: 10.3303/CET25117180.

Nicol, M. J., Fleming, C. A., & Paul, R. L. (1987). The Chemistry of the Extraction of Gold. In The extractive metallurgy of gold (pp. 831–905).

Nielsen, J. B. K., & Lampen, J. 0. (1982). Glyceride-Cysteine Lipoproteins and Secretion by Gram-Positive Bacteria. In Journal of Bacteriology. https://journals.asm.org/journal/jb.

Otwell, A.E., Callister, S.J., Sherwood, R.W., Zhang, S., Goldman, A.R., Smith, R.D., Richardson, R.E., 2018. Physiological and proteomic analyses of Fe (III)-reducing co-cultures of *Desulfotomaculum reducens* MI-1 and *Geobacter sulfurreducens* PCA. Geobiology 16 (5), 522–539. https://doi.org/10.1111/gbi.12295.

Paesa, M., Remirez de Ganuza, C., Alejo, T., Yus, C., Irusta, S., Arruebo, M., Sebastian, V., Mendoza, G., 2023. Elucidating the mechanisms of action of antibiotic-like ionic gold and biogenic gold nanoparticles against bacteria. J. Colloid Interface Sci. 633, 786–799. https://doi.org/10.1016/j.jcis.2022.11.138.

Panda, T., Deepa, K., 2011. Biosynthesis of gold nanoparticles. J. Nanosci. Nanotechnol. 11 (12), 10279–10294. https://doi.org/10.1166/jnn.2011.5021.

Pande, V., Pandey, S.C., Sati, D., Bhatt, P., Samant, M., 2022. Microbial Interventions in Bioremediation of Heavy Metal Contaminants in Agroecosystem. Front. Microbiol. 13 (May), 1–16. https://doi.org/10.3389/fmicb.2022.824084.

Pineda, Y.S., Devries, S.L., Steiner, N.C., Block-Cora, K.A., 2023. Bioleaching of Gold in Mine Tailings by *Alcaligenes faecalis*. Minerals 13 (3), 1–13. https://doi.org/10.3390/min13030410.

Pourali, P., Badiee, S.H., Manafi, S., Noorani, T., Rezaei, A., Yahyaei, B., 2017. Biosynthesis of gold nanoparticles by two bacterial and fungal strains, *Bacillus cereus* and *Fusarium oxysporum*, and assessment and comparison of their nanotoxicity in vitro by direct and indirect assays. Electron. J. Biotechnol. 29, 86–93. https://doi.org/10.1016/j.ejbt.2017.07.005.

Reith, F., Lengke, M.F., Falconer, D., Craw, D., Southam, G., 2007. The geomicrobiology of gold. ISME J. 1 (7), 567–584. https://doi.org/10.1038/ismej.2007.75.

Reith, F., Rogers, S.L., McPhail, D.C., Webb, D., 2006. Biomineralization of gold: Biofilms on bacterioform gold. Science 313 (5784), 233–236. https://doi.org/10.1126/science.1125878.

Ryan, R.P., Monchy, S., Cardinale, M., Taghavi, S., Crossman, L., Avison, M.B., Berg, G., van der Lelie, D., Dow, J.M., 2009. The versatility and adaptation of bacteria from the genus *Stenotrophomonas*. Nat. Rev. Microbiol. 7 (7), 514–525. https://doi.org/10.1038/nrmicro2163.

Sanyal, S.K., Pukala, T., Mittal, P., Reith, F., Brugger, J., Etschmann, B., Shuster, J., 2023. From biomolecules to biogeochemistry: Exploring the interaction of an indigenous bacterium with gold. Chemosphere 339 (July). https://doi.org/10.1016/j.chemosphere.2023.139657.

Segel, I.H., 1993. Enzyme Kinetics- Behaviour and analysis of rapid equilibrium and steady- state enzyme systems. In Wiley 1, 18–60.

Singh, K.K., Vaishya, R.C., 2017. Bioremediation of Heavy Metal using Consortia developed from Municipal Wastewater Isolates. SAMRIDDHI: a Journal of Physical Sciences. Eng. Technol. 9 (01), 57–66. https://doi.org/10.18090/samriddhi.v9i01.8339.

Sitnikova, K.O., Nemchenko, U.M., Voropaeva, N.M., Grigorova, E.V., Savilov, E.D., Markova, Y.A., Belkova, N.L., 2022. the Effectiveness of Biofilm Formation of Daily Cultures of Clinically significant Strains of Opportunistic Bacteria. Acta Biomedica Scientifica 7 (5–1), 119–128. https://doi.org/10.29413/ABS.2022-7.5-1.13.

Söhnel, T., Brown, R., Kloo, L., Schwerdtfeger, P., 2001. The stability of gold iodides in the gas phase and the solid state. Chem. A Eur. J. 7 (14), 3167–3173. https://doi.org/10.1002/1521-3765.

Tendenedzai, J.T., Chirwa, E.M.N., Brink, H.G., 2021. Performance evaluation of selenite (SeO_3^{2-}) reduction by *Enterococcus* spp. Catalysts 11 (9). https://doi.org/10.3390/catal11091024.

Thirumurugan, A., Ramachandran, S., Tomy, N.A., Jiflin, G.J., Rajagomathi, G., 2012. Biological synthesis of gold nanoparticles by *Bacillus subtilis* and evaluation of increased antimicrobial activity against clinical isolates. Korean J. Chem. Eng. 29 (12), 1761–1765. https://doi.org/10.1007/s11814-012-0055-7.

Tunçel, G., Göktan, D., 1990. Effect of different methods of soaking soya beans on the growth of *Bacillus cereus*, *Klebsiella pneumoniae* and *Staphylococcus aureus* in tempeh. J. Sci. Food Agric. 53 (3), 287–296. https://doi.org/10.1002/jsfa.2740530302.

Ubaldini, S., Guglietta, D., Vegliò, F., Giuliano, V., 2019. Valorization of mining waste by application of innovative thiosulphate leaching for gold recovery. Metals 9 (3). https://doi.org/10.3390/met9030274.

Vilain, S., Luo, Y., Hildreth, M.B., Brözel, V.S., 2006. Analysis of the life cycle of the soil Saprophyte *Bacillus cereus* in liquid soil extract and in soil. Appl. Environ. Microbiol. 72 (7), 4970–4977. https://doi.org/10.1128/AEM.03076-05.

Wang, J., Li, G., Yin, H., & An, T. (2020). Bacterial response mechanism during biofilm growth on different metal material substrates: EPS characteristics, oxidative stress and molecular regulatory network analysis. Environmental Research, 185(November 2019), 109451. DOI: 10.1016/j.envres.2020.109451.

Wang, X., Chen, T., Gao, C., Xie, Y., & Zhang, A. (2022). Use of extracellular polymeric substances as natural redox mediators to enhance denitrification performance by accelerating electron transfer and carbon source metabolism. Bioresource Technology, 345(October 2021), 126522. DOI: 10.1016/j.biortech.2021.126522.

Wang, Y., L., Ye, L., Chen, J., Li, Y., Zhang, Q., & Jing, C., 2022b. Identification and Characterization of Au (III) Reductase from *Erwinia* sp. IMH. JACS Au 2 (6), 1435–1442. https://doi.org/10.1021/jacsau.2c00170.

Wessel, A.K., Arshad, T.A., Fitzpatrick, M., Connell, J.L., Bonnecaze, R.T., Shear, J.B., Whiteley, M., 2014. Oxygen limitation within a bacterial aggregate. MBio 5 (2). https://doi.org/10.1128/mBio.00992-14.

Yougbare, S., Chang, T.K., Tan, S.H., Kuo, J.C., Hsu, P.H., Su, C.Y., Kuo, T.R., 2019. Antimicrobial gold nanoclusters: recent developments and future perspectives. Int. J. Mol. Sci. 20 (12). https://doi.org/10.3390/ijms20122924.

Zheng, K., Setyawati, M.I., Leong, D.T., Xie, J., 2017. Antimicrobial Gold Nanoclusters. ACS Nano 11 (7), 6904–6910. https://doi.org/10.1021/acsnano.7b02035.